minerals

MDPI

Article

Strata Movement of Gangue Grouting Filling in Subsequent Space for Coal Mining and Analysis of Its Practical Effects

Tailong An [1], Zhongya Wu [2], Jixiong Zhang [2,*], Yexian Liu [3], Gang Duan [2], Nan Zhou [2] and Hao Yan [2]

1 Inner Mongolia Autonomous Region Energy Technology Center, Energy Bureau of Inner Mongolia Autonomous Region, Hohhot 010098, China; anhongcumt@126.com
2 State Key Laboratory of Coal Resources and Safe Mining, School of Mines, China University of Mining and Technology, Xuzhou 221116, China; zhongyawu@126.com (Z.W.)
3 Shandong Energy Group XiBei Mining Co., Ltd., Xi'an 710018, China
* Correspondence: cumtzjxiong@163.com

Abstract: There is a huge amount of solid waste generated in coal resource exploitation and utilization, leading to effects on the environment and hindering sustainable development. Aiming at the difficulty of disposal of coal-based solid waste from high-yield, high-efficiency mines, this research proposed a technique of gangue grouting filling in subsequent space (GGFSS) for coal mining and explored the movement of key strata backfilled using GGFSS technique and surface deformation characteristics using theoretical analysis and a field measurement method. The results indicate that the equivalent backfilled ratio (EBR) when using GGFSS is defined as the ratio of the grouting volume to available void volume, which is mainly affected by bed separation void volume, grouting volume, and the void volume of the caving zone. Using an EBR ground control mechanical model, the changes in the displacement and bending moment of key strata with the variation of the EBR were investigated. The critical EBR for the rupture of key strata was determined to be 74.44%. On this basis, the calculation methods of equivalent mining height (EMH) and the subsidence factor of GGFSS were proposed and then a surface deformation prediction model of GGFSS was established based on the principle of the probability integration method. The predictions implied that, at an EBR greater than 75%, the surface deformation could be significantly reduced. Engineering applications verified the effect of GGFSS on the control of ground movement. In-situ measurements of concentration, density, and particle size of the filling body were all close to the those designed values: the GGFSS technique shows longer grouting duration and a larger amount of grouting and its filling body can support impervious key strata above the working face in a mine, significantly decreasing surface subsidence.

Keywords: solid waste disposal; subsequent space; gangue grouting filling; ground control; surface deformation

check for updates

Citation: An, T.; Wu, Z.; Zhang, J.; Liu, Y.; Duan, G.; Zhou, N.; Yan, H. Strata Movement of Gangue Grouting Filling in Subsequent Space for Coal Mining and Analysis of Its Practical Effects. *Minerals* **2023**, *13*, 609. https://doi.org/10.3390/min13050609

Academic Editor: Mamadou Fall

Received: 21 March 2023
Revised: 17 April 2023
Accepted: 24 April 2023
Published: 27 April 2023

1. Introduction

Stockpiling of coal-based solid wastes including coal gangue and fly ash not only occupies a lot of land but also causes serious issues relating to environmental pollution and mining safety [1]. Underground mine backfilling of coal-based solid waste can deal with a series of issues arising from the accumulation of coal-solid waste [2–4]. There is a huge amount of mining of coal under buildings, water bodies, and railways in China's coal mines. Mining with backfilling of coal-based solid wastes can control strata movement, reduce surface deformation, and protect aquifers and release the valuable coal resources under buildings, water bodies, and railways [5,6]. Meanwhile, it helps diminish the ground pressure on mining fields, which further decreases mining hazards [7,8].

Backfilled mining originated in the North Lyell Mine in Australia in 1915. After continuing exploration and practices, at the end of the 20th century, this technique has been developed into backfilling techniques including dry filling of waste rock, hydraulic filling, low-concentration tailings filling, etc. [9]. However, these techniques have disadvantages such as low efficiency, a low degree of mechanization, and high labor intensity. Entering the 21st century, China puts more emphasis on green mining philosophy, which gradually demands better backfilling effect and efficiency. In such context, the coal mine backfilling technique has witnessed rapid development. From 2002–2008, techniques including solid filling, paste filling, and super high-water filling were developed consecutively. Thereafter, to meet the demands of high-yield high-efficiency coal mine and deep coal mining, techniques including fully mechanized solid backfill mining technology, longwall-roadway cemented backfilling technology, as well as screening and backfilling integrated technology, were developed [10–12].

Nowadays, backfilling materials are subject to diversified development [13,14], while the objectives of backfilled mining have evolved from a single purpose (the disposal of solid waste from coal mines) into multiple purposes including control of overburden strata movement, surface deformation control, prevention and control of coal mine hazards, low damage to the ecological environment, and coal and geothermal energy collaborative mining. Intelligent, efficient, and functional backfilling has been considered as a primary goal for the development of coal mine backfilling techniques [15–17].

Strata movement and control during backfilled mining is always an important issue in the development of the backfilled mining technique. Huang Yanli et al. [18] established an elastic mechanical model for the overburden strata in a coal mining field that used a solid backfilling technique to determine critical conditions, ensuring that the main roof remained free from rupture. Huang Peng [19,20] et al. built a coal wall-support-filling body coupled model for roof control to reveal the roof-control mechanism underpinning the combined actions of the filling body and mine supports. Tien Trung Vu [21,22] et al. studied the stress–strain state of the rock mass and proposed a solution to prevent face spalling and roof drop. Adam Smoli'nski [23,24] et al. studied the effect of leaving waste rock in thin mining voids on coal quality. Yan Hao [25] et al. proposed the method of cracking coal mass by supercritical carbon dioxide to weaken the mine pressure in stope. Xu Jialin [26] et al. developed a partial backfilling coal mining technique for key strata control by considering both overburden strata characteristics and control demands. Chang Qingliang [27] et al. utilized the theory of beams on elastic foundations to build a mechanical model for roof rock beams in backfill mining to study those factors affecting roof strata movement and deformation during backfilled mining. Xu Mengtang [28] et al. built a roof mechanical model for backfilled mining of the longwall working face with ultra-high water-content materials to estimate the influences of factors including the length of backfilled working face on deformation and failure of key strata. Predictions of surface deformation upon backfilled mining can guide the design of technological parameters and verify the backfilling effect. Guo Guangli [29] et al. proposed a probability integration method based on equivalent mining height to evaluate the surface deformation in the case of different backfilling ratios. Zhu Xiaojun [30] et al. proposed a predictive model for superposition of the subsidence in backfilled mining zone based on a conventional probability integration method. Wang Lei et al. [31] used physical simulations and borehole observations to reveal the evolution of overburden strata structure when using backfilled mining and established a surface subsidence prediction model for compacted solid backfilled mining.

To sum up, there have been multiple mature developed coal mine backfilling techniques including solid backfilling, paste backfilling, high-water material filling, longwall-roadway cemented backfilling, and the overburden bed separation grouting technique and allied theories. However, due to the limits of backfilling efficiency and disturbance caused during coal mining, these backfilling techniques and theories are unable to be completely applicable to large-scale, high-capacity, high-efficiency coal mines. In the existing filling mining, coal mining and backfill processes operate in parallel or in succession in the same space. The filling process increases the length and complexity of the mining process on the working face and reduces the efficiency of coal mining. At the same time, the existing filling technology only uses the mining space of coal seam, and fails to make full use of the space and pores in the goaf. In order to solve the above problems in backfill mining, Yin Wei et al. [32] proposed the method of backfilling collaborating with the caving fully-mechanized mining. This method arranges caving and backfill sections in the same working face, which ensures the backfill capacity and improves the coal mining capacity. Zhang Qiang et al. [33] designed the solid intelligent filling control program and system, and proposed the working condition characterization and self-identification control method. V. Tran et al. [34–36] used the intelligent model to predict the strength and flow characteristics of cemented paste backfills. In order to solve the above problems in filling mining, this paper proposes the GGFSS based on the idea of "mining first, filling later". This new filling technology can inject millimeter-level gangue slurry into the void in caving zone and fractured zone, with a low cost, flexible layout, and has no space–time interference between filling and coal mining, which can realize efficient treatment of gangue, control rock movement, and reduce surface subsidence. The technique of gangue grouting filling in subsequent space (GGFSS) for coal mining as a new backfilled mining technique was developed based on overburden bed separation grouting technology. GGFSS technique added water to millimeter-scale coal gangue particles to prepare a slurry, which is then transported to the subsequent space of a coal mine with the aim of disposing of all gangues in underground mines. At present, this technique is in its infancy. The theoretical foundation and technological systems remain in the developmental stage. At present, the GGFSS has only been applied in a few coal mines such as Sangshuping No. 2 Well and Huangling No. 2 Well [37,38], and there is no relevant research on shallow buried and kilometer mine. When the GGFSS is applied in the mine with different buried depths, the suitable grouting hole layout is different. For shallow buried mines, drilling and filling from the ground down is a relatively economical and efficient way. For mines buried more than 1000 m, due to the low efficiency of gangue lifting and the difficulty and high cost of ultra-deep drilling and maintenance, the grouting filling method of drilling holes through the coal pillar to the nearby goaf is more suitable. In this paper, principles, and technological keys of GGFSS technique were expounded. Aiming at the research of strata movement of GGFSS, an EBR concept was proposed. Based on this, the ground control mechanical model of GGFSS was established and key parameters of the probability integration method for surface deformation were rectified to form a GGFSS surface deformation prediction model. Finally, a field measurement analysis of engineering application effect of GGFSS technique was performed.

2. GGFSS Technique

2.1. Principle of GGFSS

The GGFSS technique, when used in coal mines, entails the addition of water to millimeter-scale coal gangue particles to prepare a gangue slurry, which is transported to the subsequent space in coal mines with the aim of disposing of gangue in underground mines. Without affecting the production efficiency of the mining operations underway at the working face, it can realize the large-scale treatments of coal gangues and control of strata movement in underground mines. The subsequent space of coal mines refers to the zones including caving zone, crack zones, and bed separation zone, which are generated by overburden strata. The technological principle of GGFSS is shown in Figure 1.

Compared with traditional backfilled mining techniques, the advantages of GGFSS techniques used in coal mines mainly include: the backfilled zone is the space of the coal mining working face, and the backfilling does not affect coal mining efficiency; the slurry preparation transportation system is quite well developed, which requires less labor, low investment, and a short construction period; the backfilling positions are flexibly arranged, which shows strong adaptability, and is free from restrictions of coal seam mining methods and geological conditions; gangue grouting filling is rapid and can fulfill multiple parallel operations; and gangue slurry is transported by pipelines, which demonstrates flexibility is practice.

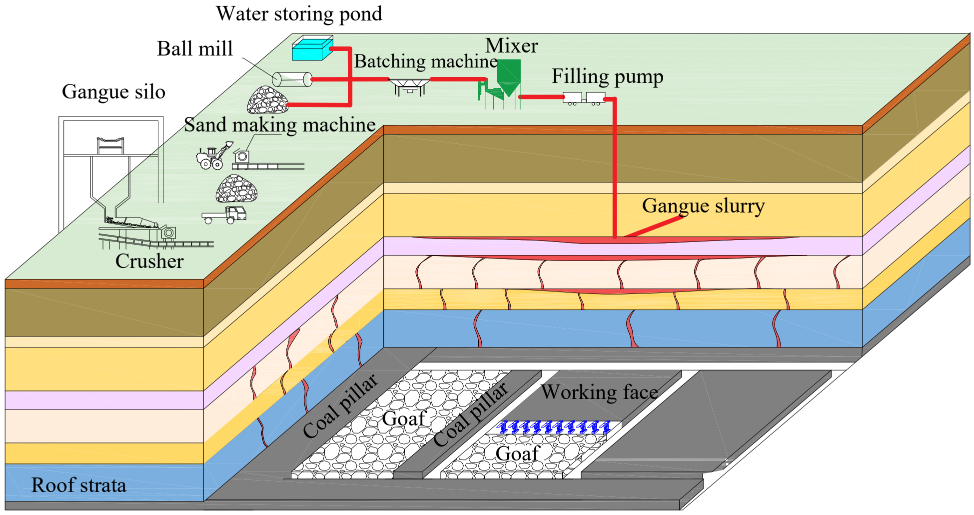

Figure 1. General conception of GGFSS in coal mining.

The GGFSS has the following limitations: (1) gangue needs to be broken into millimeter-level filling material, which requires multi-stage crushing; (2) generally, the hardness coefficient of gangue should be between 4 and 8.5, the gangue with a small hardness coefficient is easy to deform but not easy to break, and the gangue with large hardness coefficient is easy to break, but the loss of equipment is faster; and (3) the preparation of gangue slurry consumes a lot of water, so it is not suitable to be used in mines where water is scarce or mine water cannot be recycled.

In order to reduce the cost of the GGFSS, the cementing material of the filling material is greatly reduced or directly eliminated so that the flow and solidification performance of the filling material is quite different from that of cemented paste backfill. For the filling material without cementing material, it will not solidify itself, but will gradually consolidate under the pressure of the overlying rock in the goaf. For the filling material with cementing material, the flow and solidification characteristics are different according to the type and content of cementing material. However, in order to achieve pumping effect, the bleeding rate of filling materials is generally required to be 5~20% and the slump flow is greater than 200 mm.

2.2. Technological Key to GGFSS

To realize GGFSS, it is necessary to develop grouting filling materials with excellent transportation performance, and investigate the structural characteristics and spatiotemporal evolution of pores in the subsequent space, investigate the migration and diffusion of gangue slurry in the subsequent space, construct a ground control method of GGFSS, and form an accurate and well-developed monitoring system to assess the filling effect. Furthermore, high-efficiency disposal and ground control of solid wastes can be realized.

As the GGFSS technological process differs from traditional paste filling and solid filling, the overburden strata movement law of GGFSS shows specificity, and traditional ground control theory is difficult to apply directly. In comparison with traditional backfilled mining technique, as the backfilled zone of GGFSS is irregular, filling effects are unable to be characterized by the existing backfilled ratio or filling ratio. Therefore, it is necessary to establish a suitable EBR index for analyzing overburden movement and surface deformation characteristics of GGFSS, which can be used to guide engineering practice.

3. Ground Control Mechanical Model of GGFSS

3.1. EBR Mechanical Model

After coal seam mining, the overburden strata will reach a new equilibrium. The overburden strata can be divided into a caving zone, a crack zone, and a bending subsidence zone. As illustrated in Figure 2, due to the differences of mechanical properties of different rock strata and bulking characteristics of crushed gangues, there are many bed-separation voids and caving zone voids formed between rock strata. GGFSS takes the void volume V_3 as the difference between coal seam mining volume V, and surface subsidence space volume V_1 and unavailable void volume V_2, which consists of the void volume V_1 of the crack zone and the void volume V_f of the caving zone.

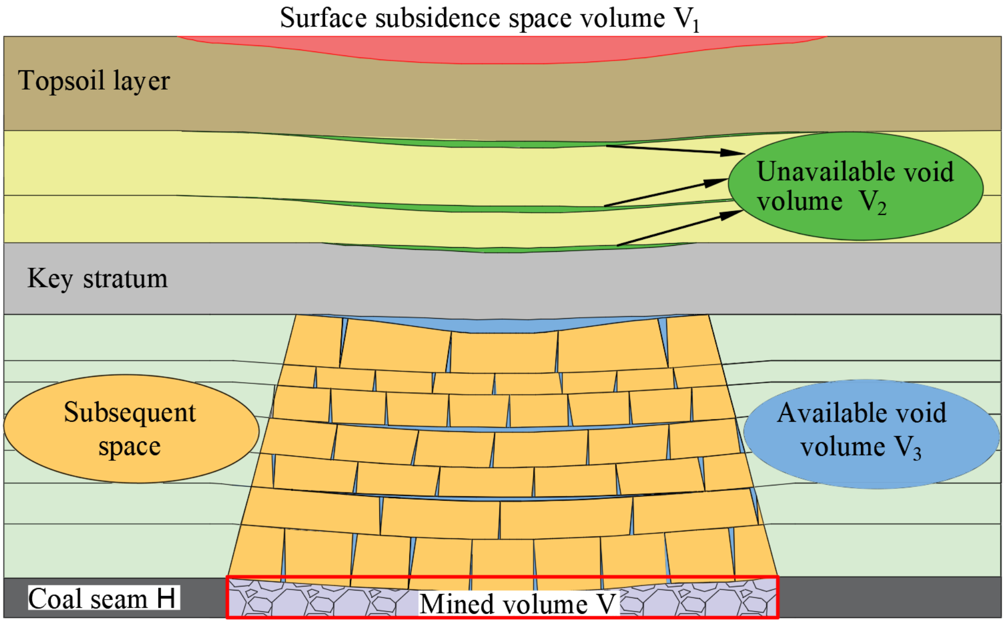

Figure 2. The EBR model for surface deformation when using GGFSS.

H denotes the mining thickness of the coal mining working face.

The EBR is defined as the ratio of the grouting volume V_g to available void volume V_3, as given by

$$\varphi = \frac{V_g}{V_3} = \frac{V_g}{V - V_1 - V_2} = \frac{V_g}{V_l + V_f}, \tag{1}$$

where, φ represents the EBR, V_g is the grouting volume, V_3 denotes the available void volume, V is the volume of the coal seam mining working face, V_1 refers to the surface subsidence space volume, V_2 is the unavailable void volume, V_l denotes the void volume of the crack zone, and V_f stands for the void volume of the caving zone.

Before the rupture and movement of key strata, a large part of the bed-separation zone in the floor strata reaches its maximum extent, the volume of the bed separation zone in the crack zone can be calculated based on subsidence deformation of subjacent strata. The void volume of the caving zone can be determined according to the void volume of the caving zone and void fraction. Hence, the factor influencing the EBR mainly comprises the void volume of bed separation, grouting volume, and the void volume of the caving zone, as shown in Figure 3.

Based on the EBR in the case of different grouting amounts, all strata in the whole zone for slurry backfilling below key strata form a bulk filling body. According to the Winkler foundation assumption theory, key strata are simplified into a beam with both ends fixed on an elastic foundation. The beam length is the length of goaf. Using uniformly distributed loads in place of the upper part of the beam, the mechanical model spanning from coal seams to key strata was established. The structure of the overburden strata subjected to grouting backfill grouting is shown in Figure 4. The key strata mechanical model is depicted in Figure 5.

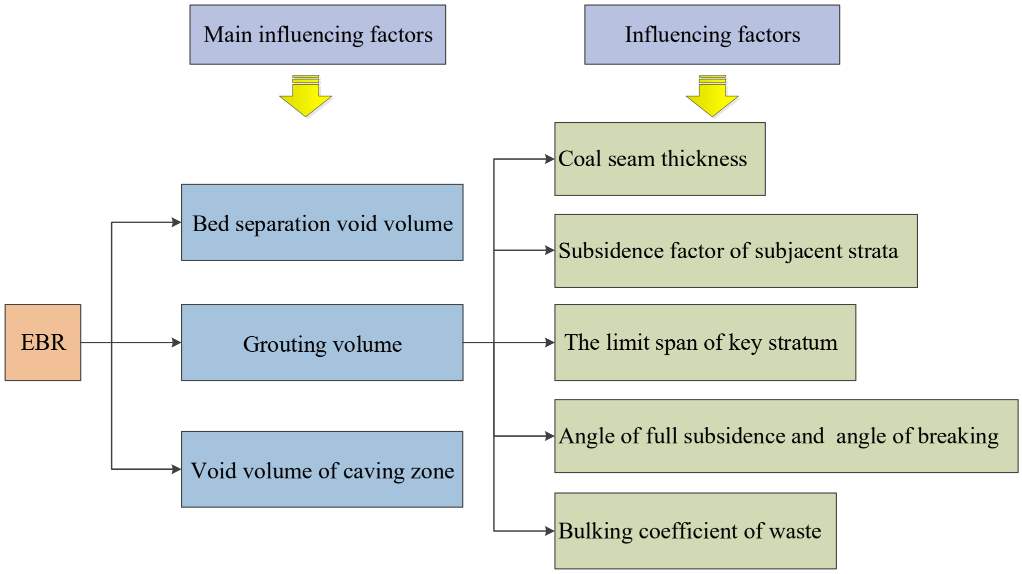

Figure 3. Factors influencing of the EBR.

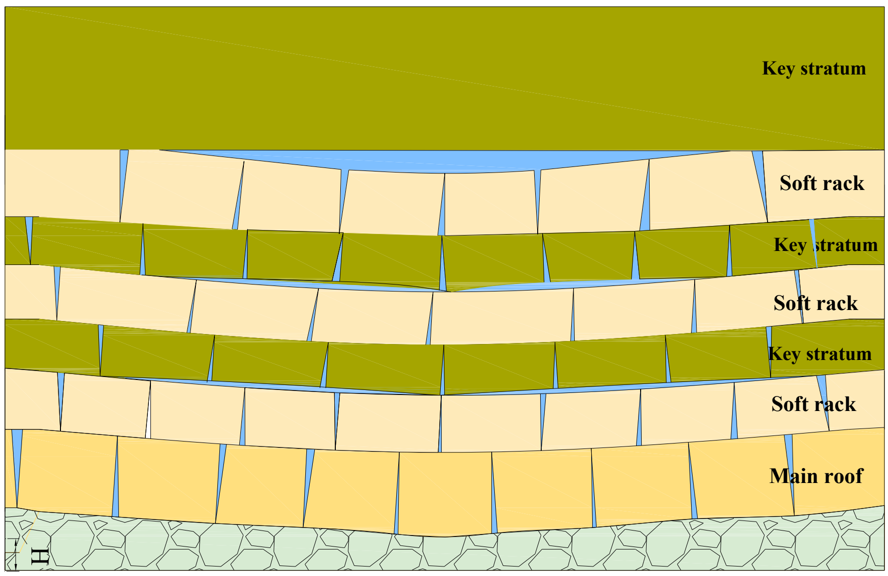

Figure 4. Overburden structure.

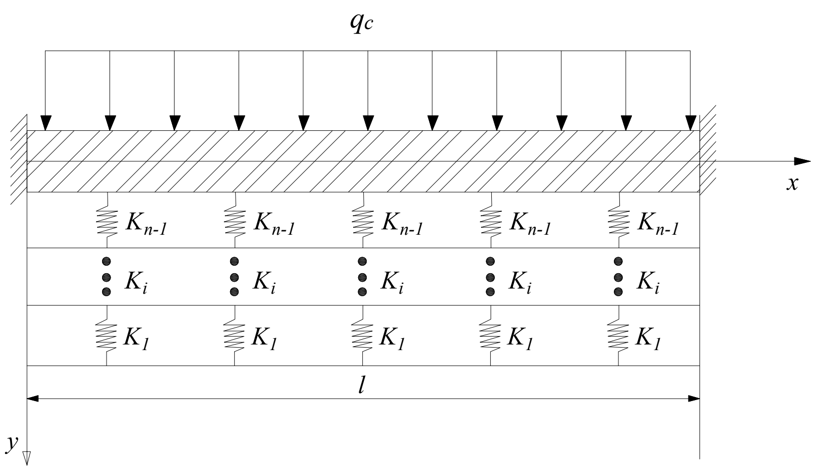

Figure 5. Mechanical model of key strata.

After backfill grouting, the differential equation for the deflection of key strata q_c is given by:

$$E_n I_n \frac{d^4 w(x)}{dx^4} + kw(x) = q_c, \quad (2)$$

where, E_n and I_n represent elastic modulus and moment of inertia, respectively; k refers to the overall elastic foundation coefficient of superimposed subjacent strata. Using eigenvalue $\alpha = \sqrt[4]{\frac{k}{4E_n I_n}}$, Equation (2) is solved to give:

$$w(x) = \frac{q_c}{k} + e^{-\alpha x}[d_3 \cos(\alpha x) + d_4 \sin(\alpha x)] + e^{\alpha x}[d_5 \cos(\alpha x) + d_6 \sin(\alpha x)], \quad (3)$$

Coefficients d_3, d_4, d_5, and d_6 can be solved based on the following boundary conditions:

$$\left\{ \begin{array}{l} w(0) = 0,\ w(l) = 0 \\ \theta(0) = 0,\ \ \theta(l) = 0 \end{array} \right\}, \quad (4)$$

The relationship of rotation angle θ, bending moment M, and shearing force Q with the deflection $w(x)$ at any arbitrary cross-section through the beam is expressed as:

$$\left\{ \begin{array}{l} \theta(x) = \frac{dw(x)}{dx} \\ M(x) = -EI\frac{d^2 w(x)}{dx^2} \\ Q(x) = -EI\frac{d^3 w(x)}{dx^3} \end{array} \right\}, \quad (5)$$

3.2. The EBR-Based Strata Movement Mechanical Model

3.2.1. The EBR of Different Backfill Grouting Zones

Based on prevailing geological conditions, the number of bed separation voids can be determined. The void volumes of the caving zone and bed separation can be calculated using the subsidence deformation of subjacent strata, the volume of the caving zone, and void fractions. On this basis, available void volume can be obtained. According to different grouting amounts, the EBR of different backfill grouting zones and the critical EBR that ensures key strata free from rupture are calculated, respectively.

① Calculation of void volume

The void volume of the caving zone is calculated as:

$$V_f = Lb_0 H_f \mu = Lb_0 \left(\frac{100 \sum H_m}{4.7 \sum H_m + 19} \pm 2.2 \right) \left(1 - \frac{1}{K_p} \right), \quad (6)$$

where, L represents the length of the mined zone, b_0 denotes the length of the coal mining working face, H_f is the height of the caving zone, μ is the porosity of the caving zone, H_m is the mining height, and K_p is the bulking coefficient of crushed gangue.

The void volume of bed separation is the sum of maximum void volume of bed separation and the void volume of the remaining strata. The void volume of the remaining strata accounts for one-third of the maximum void volume of upper strata before being ruptured, while the void volume of bed separation is given by:

$$V_l = V_{l1} + \frac{1}{3}(V_{l2} + V_{l3} + \cdots + V_{l6}), \quad (7)$$

where, V_{l1} is the maximum void volume of bed separation; V_{li} denotes the void volume of remaining strata (= 2, 3, 4, 5, 6). The overall void volume of the subsequent space is $V_s = V_l + V_f$.

② The relationship between the EBR and elastic foundation coefficient

The relationship between elastic modulus, the backfilled ratio, and elastic foundation coefficient is:

$$\left\{ \begin{array}{l} \sigma = K_b w \\ \varepsilon = w/h_b \\ E = h_b K_b \\ \varphi = (h_b - \Delta)/h_b \\ \Delta = \sigma/K_b \end{array} \right\}, \quad (8)$$

where, K_b is the foundation coefficient of the backfilled zone, w refers to the deflection of key strata, h_b is the height of the backfilled zone, Δ represents the final subsidence of the backfilled zone, E denotes the elastic modulus of key strata, and σ is the overburden load of the backfilled zone.

The deformation of key strata depends on the final deformation of filling body. The elastic foundation coefficient is equal to the ratio of the elastic modulus and thickness of foundations, hence, the EBR of subsections can be expressed as:

The EBR of the section ranging from the backfill grouting layer to the caving zone is given by:

$$\varphi = 1 - \frac{q_c(\sum_i^n \frac{h_i}{E_i} + \sum_i^m \frac{h_{si}}{E_g} + \frac{h_f}{E_g})}{h_b}, \quad (9)$$

The EBR of the section ranging from the backfill grouting layer to bed separation zone is therefore:

$$\varphi = 1 - \frac{q_c(\sum_i^n \frac{h_i}{E_i} + \sum_i^m \frac{h_{si}}{E_g})}{h_b}, \quad (10)$$

where, E_i refers to elastic modulus of each stratum in the backfilled zone, E_g denotes the elastic modulus of gangue slurry in the bed separation zone and the caving zone, h_s is the height of bed separation, h_f represents the EMH backfilled in the caving zone, and h_i is the height of the backfill grouting layer.

The gangue slurry backfilled zone can be divided into seven zones according to actual grouting amounts. These seven zones are within the area covering the bed separation zone and medium-grained conglomerate which are both below the boreholes, and the caving zone. The backfill grouting layer includes respectively, medium-grained conglomerate, coarse-grained sandstone, siltstone, medium-grained sandstone, siltstone, and coarse-grained sandstone.

Integrating Equations (9) and (10), the EBR corresponding to each filling stratum can be obtained (Table 1).

Table 1. EBR corresponding to filling strata.

Strata	Filling Height/m	Foundation Coefficient/kN/m^3	EBR/%	Theoretical Grouting Volume/m^3
Coarse-grained sandstone	26.07	1502	φ_1 = 21.67	21,689.54
Siltstone	38.65	2515	φ_2 = 30.25	30,277.27
Medium-grained sandstone	55.02	3012	φ_3 = 38.83	38,865.01
Siltstone	73.52	3555	φ_4 = 47.41	47,452.74
Coarse-grained sandstone	92.76	4089	φ_5 = 55.98	56,030.46
Medium-grained conglomerate	121.71	5080	φ_6 = 75.34	75,407.92
Caving zone	136.97	53,605	φ_7 = 95.07	95,155.71

The backfilled coal mining working face is the 3^{-1}801 working face with a width of 246 m and an advancing length of 2775 m in a coal mine in Inner Mongolia, China. The main coal seam was 3^{-1} coal, with a coal seam dip angle of 1~3°, an average thickness of 5.7 m and a coal seam burial depth of 655~670 m. The immediate roof of the 3^{-1} coal seam contains soft to semi-hard rock strata; while the main roof of the 3^{-1} coal seam rocks is classified as semi-hard strata. Table 2 summarizes the lithology of the coal mining working face roof.

Table 2. Lithology of the 3^{-1}801 working face roof.

Roof Type	Lithology	Average Thickness/m	UCS/MPa
Immediate roof	Sandy mudstone Siltstone	2.09 3.6	31.99
Main roof	Medium-grained sandstone Grit sandstone Medium-grained sandstone	5.695 25.85 16.36	17.14

The height of the caving zone is known to be 14.6 m, the bulking coefficient of the waste is 1.10, the length of the goaf is 300 m, the angle of breaking for the overburden strata is 68°, the angle of full subsidence is 47° and the subsidence factor of overburden strata is 62.5%. According to Equations (6) and (7), the void volumes of the caving zone and the bed separation zone are calculated to be 35,592 m^3 and 59,563 m^3, respectively, while the overall void volume of the subsequent space is 95,156 m^3. Based on the relationship of elastic foundation coefficients, the EBR of the full subsequent space is determined to be 95.07%.

3.2.2. Displacement Analysis of Key Strata

It can be assumed that there are m bed separations generated in n strata layers, the deflection of the m-1th hard rock layer is:

$$\left\{ \begin{array}{l} B_i = H_m - h_{d_i}(L - K_{pi}) - W_i,\ i = 1,2,\cdots,m-1 \\ B_m = W_m,\ i = m \end{array} \right\} \quad (11)$$

where, B_i is the height of bed separation under each hard rock stratum, W_i is the deflection of the ith hard rock layer when mining using a caving method, K_{pi} is the comprehensive bulking coefficient of all strata below the ith key stratum, and h_{d_i} hdi denotes the distance between each key stratum and the coal seams.

The differential equation for the deflection of key strata mining using the caving method is:

$$W_{\mathrm{i}}(x) = \frac{q_i}{24E_iI_i}x^4 + d_1x^3 + d_2x^2 + d_3x + d_4, \quad (12)$$

where, I_i represent moment of inertia of the ith key stratum, and q_i refers to the load above the ith key stratum.

The EMH of the caving zone backfilled refers to the difference between the height of the caving zone and the height of compacted gangue in the backfilled zone. The height of the caving zone can be calculated according to the empirical formula and the EMH of the caving zone backfilled h_f is given by:

$$h_f = H_f(1 - \zeta), \quad (13)$$

where, h_f is the EMH of the caving zone when backfilled, and ζ represents the compaction coefficient of the collapsed gangue.

The foundation coefficients corresponding to EBR are substituted into Equations (11)–(13), the bending deformation of key strata with different EBRs can be obtained, as illustrated in Figure 6.

As shown in Figure 6, the maximum deflection of key strata is located at the central part of the backfilled zone. The maximum deformation of the central part of key strata mining using the caving method is 205.56 mm. As the EBR increases, the deflection of key strata decreases. Compared with the caving method, the changes in the deformation of key strata corresponding to the EBR in the range of 21.67% to 55.98% are negligible. When the

EBR is 75.34% and 95.07%, the maximum deformation of key strata is reduced by 58.88 mm and 19.75 mm, respectively; when the EBR is 95.07%, the maximum deformation of key strata is decreased by 185.81 mm compared with that of the caving method, at this time, the backfill slurry can ensure that key strata remain free from rupture.

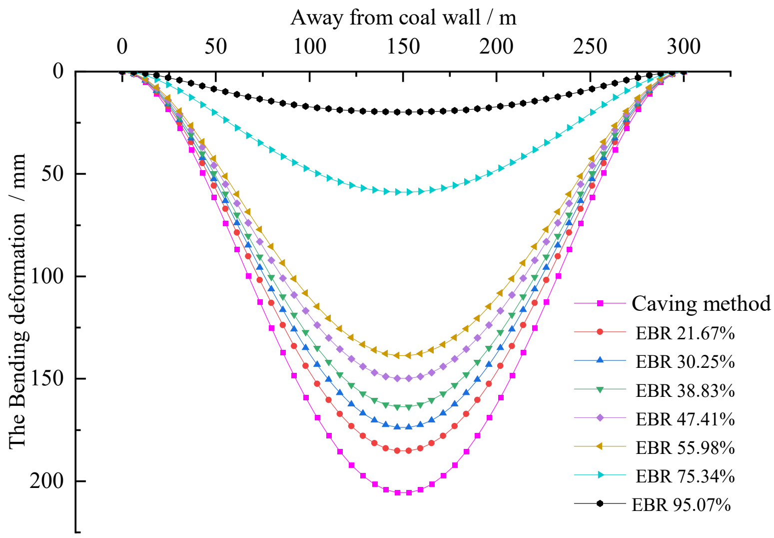

Figure 6. Bending deformation of key stratum under different EBRs.

3.2.3. Bending Moment of Key Strata

Taking the strata of the backfilled zone as a whole, the bending moments of key strata in the case of different EBRs can be calculated (Figure 7).

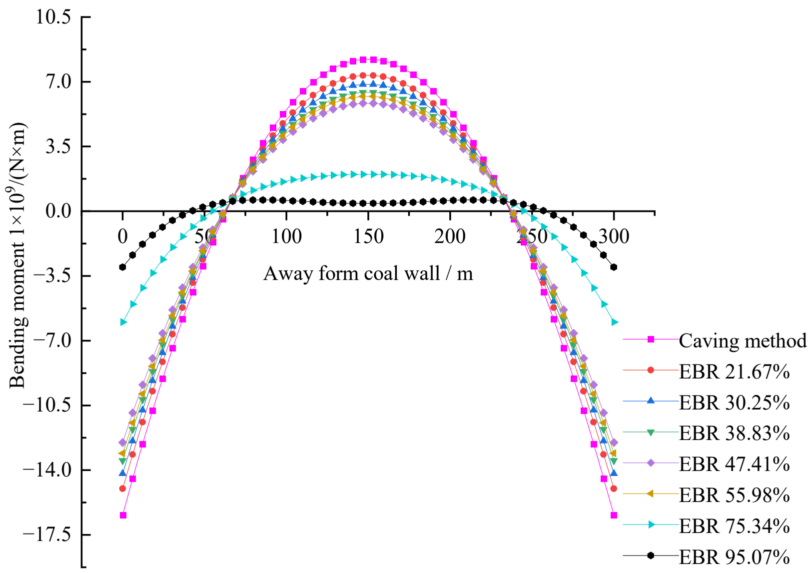

Figure 7. Bending moments of key stratum under different EBRs.

As shown in Figure 7, the bending moments of key strata at both ends of the beam are maximized, the bending moment of the upper part of the fixed-support end subjected to tension is negative. The lower part of the central zone subjected to tension shows a positive bending moment. With the increase of the EBR, the bending moment on the key strata decreases. When the EBR is between 21.67%–55.98%, the maximum tensile stress is approximately 34 Mpa, which is much greater than the allowable stress (15 Mpa). When the EBR is 75.34% and 85.07%, the maximum bending moments at both ends of key strata are -6.01×109 Nm and -3.02×109 Nm, respectively. While the maximum tensile stresses on both the ends are 13.5 Mpa and 6.9 Mpa separately. Hence, when the EBR exceeds 75.34%, the maximum tensile stress of key strata is less than the allowable stress. With the increase in the EBR, the effect of grout backfilling on the control of key strata is enhanced.

In summary, the critical EBR needed to ensure that the key strata remain free from rupture is 74.44%. When the EBR is greater than 74.44%, the deformation of key strata is reduced, the maximum tensile stress also decreases, rupture does not occur in key strata, therefore, the design value of EBR should be greater than 75%.

4. Surface Deformation When Using GGFSS

4.1. Prediction of Surface Deformation

At present, there is no surface deformation prediction method applicable to GGFSS. In the present research, a traditional surface deformation probability integration method is proposed. The EMH can be solved based on the EBR and then predictive parameters of a virtual caving method at variable mining heights are used to predict the surface deformation of GGFSS.

4.1.1. The EMH of GGFSS

There is a certain crack space which is not backfilled and compacted in the subsequent space of coal mines. The coefficient of the crack space is characterized by the difference between the bulking coefficient of broken rocks and the compaction coefficient of the gangue backfilling body. On this basis, the EMH H_d is obtained as follows:

$$H_d = H - H\varphi(k_1 - k') = H - H\frac{V_g}{V - V_1 - V_2}(k_1 - k'), \quad (14)$$

where, H_d refers to the EMH of GGFSS, denotes the mining thickness of the coal mining working face, k_1 represents the bulking coefficient of rock strata in the caving zone, k' is the compaction coefficient of GGFSS, and the unavailable void volume $V_2 = VC$. According to the surface deformations calculated under conditions of mining using the simulated caving method, the unavailable porosity C of the bending subsidence zone is about 0.08.

4.1.2. Key Parameters of Surface Deformation

The relationships between the subsidence prediction parameters under the two conditions (using GGSFF and the total caving method) were analyzed successively.

① The subsidence factor

The subsidence factor denotes the ratio of the maximum surface subsidence to the mining height of coal seams under the condition of full mining disturbance. Its key lies in determining the maximum surface subsidence after coal seam mining. The maximum surface subsidence is dependent on the mining height of coal seams, and the residual bulking coefficients of the caving zone, the crack zone, and bending subsidence zone. Its calculation is as follows:

$$W_c = H_\mathrm{d} - H_1(k_1 - 1) - H_2(k_2 - 1) - H_3(k_3 - 1), \quad (15)$$

where, W_c is the maximum surface subsidence when mining using the total caving method; H_1, H_2, and H_3 represent the heights of the caving zone, crack zone, and bending subsidence zone respectively; k_2 and k_3 separately denote the residual bulking coefficients of the crack zone and bending subsidence zone,

$$W_g = H_d - H_2'(k_2' - k') - H_3'(k_3' - k'), \quad (16)$$

where, W_g is the maximum surface subsidence value when using GGFSS; H_2' and H_3' are the heights of the crack zone and bending subsidence zone, respectively, when using GGFSS; k_2' and k_3' represent the residual bulking coefficients of the crack zone and bending subsidence zone in the case of using GGFSS, respectively.

As the bulking coefficients of the crack zone of overburden strata and bending subsidence zone are small, the bulking coefficients of the crack zone of overburden strata and bending subsidence zone when mining using the total caving methods and GGFSS with EMH can be deemed approximately equal. Hence, Equation (17) can be used to express the relationship between the surface subsidence factor obtained using the total caving method and surface subsidence factor when using GGFSS.

$$q_g = q_1 - \left[\begin{array}{l} H_2'(k_2 - k') - H_3'(k_3 - k') \\ -H_1(k_1 - k') - H_2(k_2 - k') \\ -H_3(k_3 - k') \end{array} \right] / H_d, \tag{17}$$

q_1 is the surface subsidence factor of the total caving methods.

② The tangent value of the primary influencing angle tanβ

The tangent value of the primary influencing angle tanβ for the surface deformation when using GGFSS is decreased by 0.1 to 0.3 compared with the total caving method under different EBR conditions.

③ Other parameters

Horizontal movement coefficient b, the inflection point offset S, and the propagation angle of primary mining impact θ_S are subjected to smaller influences under backfill grouting. Therefore, surface deformation parameters of all the caving methods were selected.

4.2. Surface Deformation Characteristics

4.2.1. Prediction Scheme and Parameter Selection of Surface Deformation

① Surface subsidence prediction scheme

According to the surface deformation prediction model based on the EBR, nine types of surface deformation prediction schemes in the case of different EBRs (0%, 20%, 40%, 60%, 70%, 75%, 80%, 85%, and 90%) were designed. On that basis, the changes in the surface subsidence value s, surface horizontal deformation e and slope deformation i were determined.

② Parameter selection of surface subsidence prediction

Field measurement data of surface deformation of the strata when using the caving method in the 3^{-1}101 working face in a coal mine from inner Mongolia, China were analyzed. The location of this mine is shown in Figure 8. RTK real-time positioning monitoring system was used to monitor surface subsidence and deformation values. The parameters selected for surface deformation prediction of the 3^{-1}801 working face included: the subsidence factor q_g of 0.34, horizontal movement coefficient b of 0.35; the tangent value of the primary influencing angle $\tan\beta$ of 2.15; the propagation angle of primary mining impact θ_S of 90°; and the inflection point offset S of 0.036H.

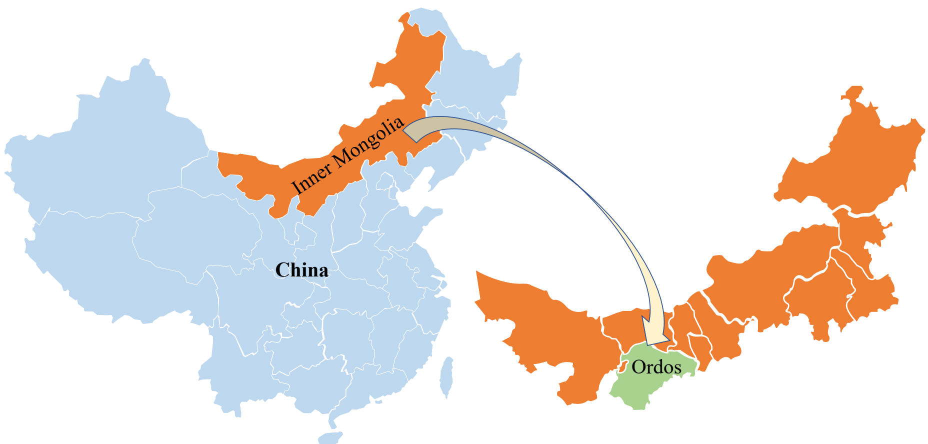

Figure 8. Mine location map.

4.2.2. Predicted Results of Surface Deformation Characteristics

① Surface subsidence when using GGFSS

Table 3 and Figure 9 show that surface subsidence decreases with the increase in the EBR; when the EBR is increased from 70% to 75%, surface subsidence demonstrates a significant reduction and the area of the subsidence basin that takes a surface subsidence of 220 mm as the delimiting isoline also decreases significantly. The results indicate that in the case of the EBR below 75%, the backfill slurry plays a limited role in controlling rock strata: the rupture of overburden strata still occurs; when the EBR is higher than 75%, backfill slurry exerts a beneficial supportive effect on the overburden strata. As the EBR increases, the better the integrity of key strata, the smaller the surface subsidence.

Table 3. Maximum subsidence under different EBRs.

EBR/%	Maximum Subsidence/mm	Area of Subsidence Basin/km^2
0	1506	1.89
20	1408	1.88
40	1289	1.79
60	1083	1.69
70	928	1.58
75	553	0.95
80	383	0.72
85	289	0.56
90	227	0.49

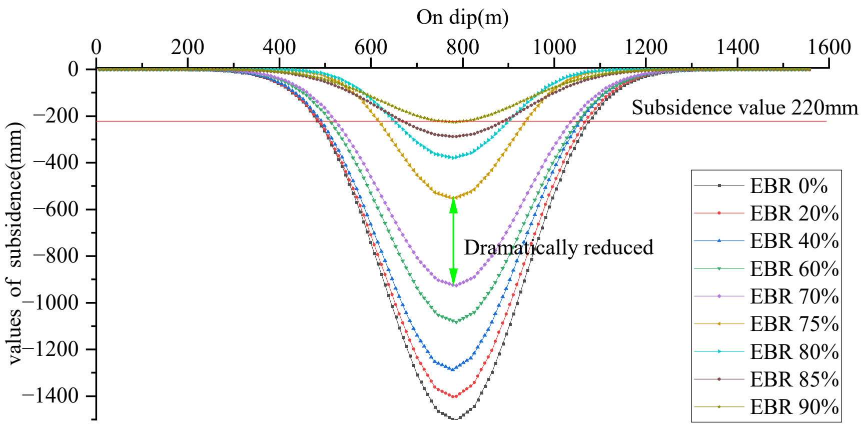

Figure 9. Surface subsidence under different EBRs.

② Surface slope deformation when using GGFSS

According to Table 4 and Figure 10, with the gradual increase of the EBR, the extremum value of surface slope deformation shows a decreasing tendency; when the EBR is increased from 70% to 75%, the slope deformation demonstrates a sharp decrease; thereafter, the decrease of the slope deformation slows. This is akin to the trend in surface subsidence data.

Table 4. Maximum slope deformation under different EBRs.

EBR/%	Slope Deformation I (mm/m)	
	Horizontal Direction	Vertical Direction
0	4.4	3.2
20	4.2	3.1
40	3.9	2.9
60	3.5	2.6
70	3.0	2.3
75	2.0	1.8
80	1.6	1.3
85	1.3	1.0
90	1.1	0.8

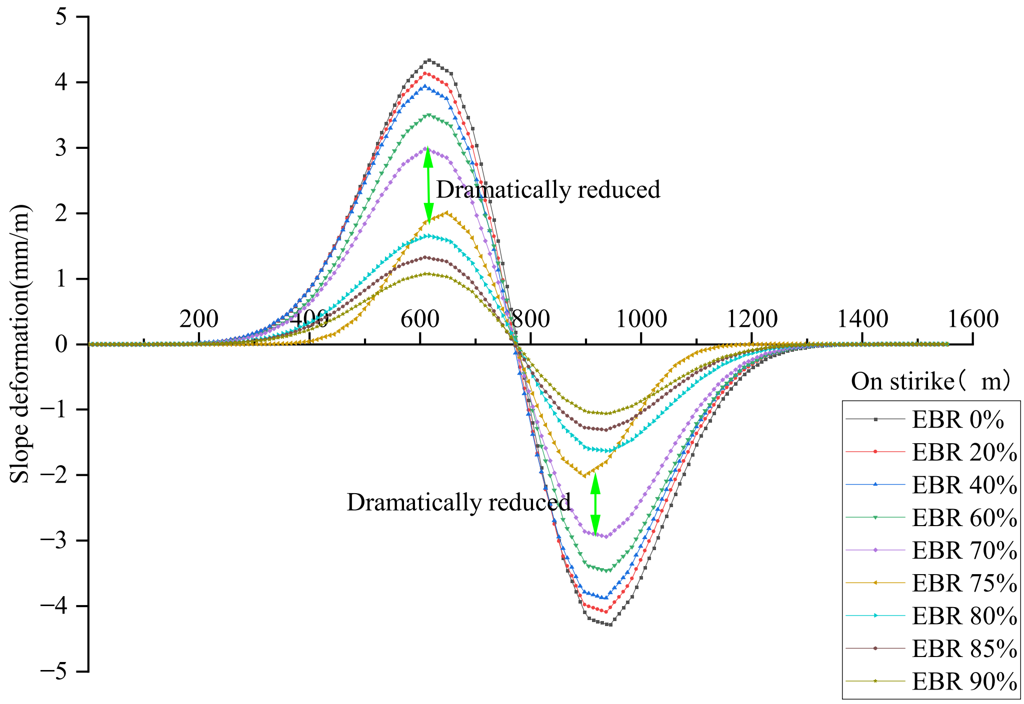

Figure 10. Surface slope deformation under different EBRs.

③ The surface horizontal deformation of GGFSS

Table 5 and Figure 11 show that as the EBR gradually increases, the extremum value of surface horizontal deformation tends to be reduced. When the EBR is increased from 70% to 75%, the maximum deformation of surface horizontal deformation is sharply decreased by about 35%. When the EBR is greater than 75%, the decreasing amplitude of the extremum value of surface slope deformation becomes smaller. These data show that, when the EBR is 75%, the gangue slurry exerts a favorable supporting effect on the subsequent space, ensuring the integrity of key strata. This is akin to the trends in surface subsidence and surface slope deformation data.

Table 5. Maximum horizontal deformation under different EBRs.

EBR/%	Horizontal Deformation i mm/m	
	Horizontal Direction	Vertical Direction
0	2.9	1.9
20	2.7	1.8
40	2.5	1.7
60	2.3	1.5
70	2.0	1.4
75	1.3	0.9
80	1.0	0.8
85	0.8	0.6
90	0.7	0.5

The aforementioned analysis implied that, when the EBR exceeds 75%, surface subsidence, surface horizontal deformation, and slope deformation all decrease significantly, and the key strata do not rupture. Given a certain safety coefficient and backfilling efficiency, the design value of EBR for this particular coal mine is 85%.

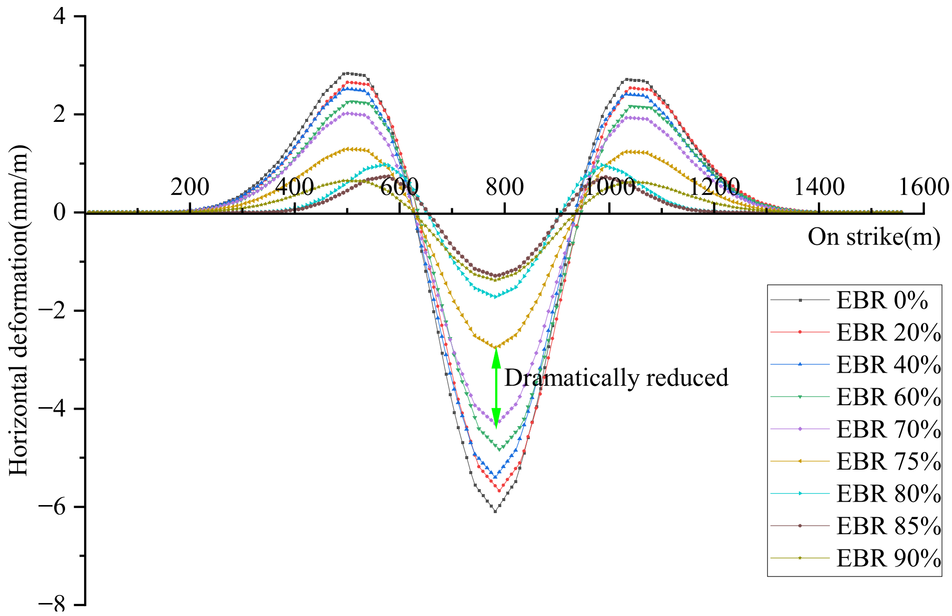

Figure 11. Surface horizontal deformation under different EBRs.

5. Engineering Application of GGFSS

5.1. Design of Gangue Backfilling Schemes

The GGFSS technique has been applied to the $3^{-1}801$ working face in a coal mine in Inner Mongolia, China. The key to backfilling scheme design includes the backfill grouting layer and borehole arrangement used for grouting.

5.1.1. Backfill Grouting Layer

When the working face is advanced to 2800 m, key strata still do not show significant bending subsidence. At this moment, the subsequent space of the $3^{-1}801$ working face theoretically reaches the maximum. As shown in Figure 12, the 51-m thick medium sandstone layer, lying 131 m above the 3^{-1} coal seams is the key stratum to be controlled, namely, the grouting layer of GGFSS.

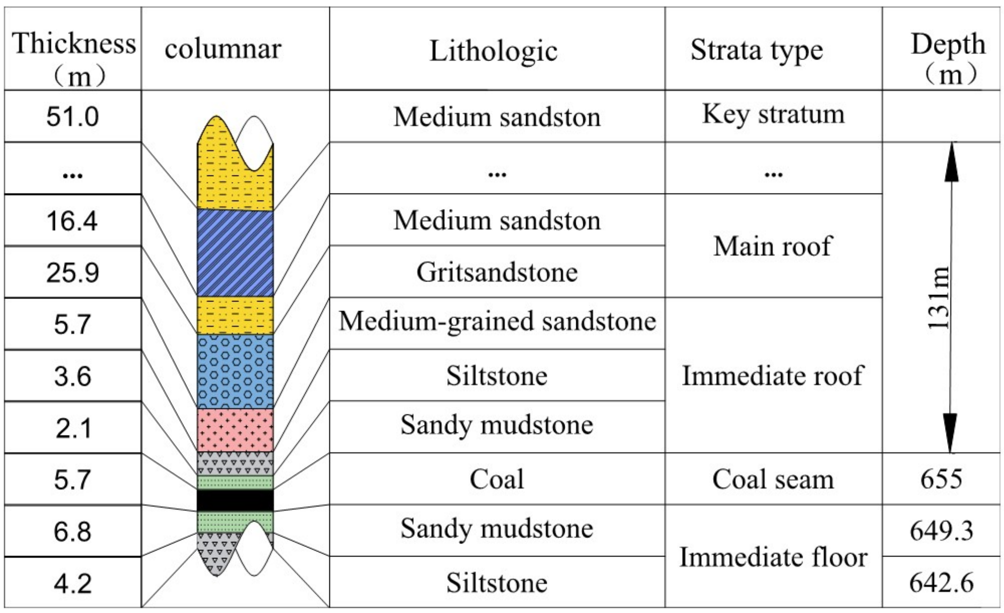

Figure 12. Borehole columnar section.

5.1.2. Arrangement of Backfill Grouting Boreholes

Through analysis, the void fractions of the subsequent space under creep effects are in the range of 20%–40%. Hence, the radial depth of the grouting diffusion zone is set to 0.935–1.492. The designed slurry mass concentration is 60%, one-third of the gangue crushed to diameter below 2 mm, and two-thirds of the gangue crushed to diameter below 0.15 mm. Under extremum conditions, gangue slurry diffuses to the bottom of the subsequent space, the diffusion radius of gangue slurry is 122.7 m to 195.9 m, and is set to 318.6 m under extremum conditions. To ensure optimal grouting effect, the distance between adjacent boreholes is set to 300 m.

Boreholes at the grout backfilled zone were arranged along the grout backfilling working face, which are situated at the center of the working face. The nine groups of boreholes in the 3^{-1}801 working face were designed. The arrangement and order of grouting of the boreholes are shown in Figure 13. The final borehole is 522 m from the surface, and the borehole bottom is 300 m. The diameter of the borehole is 127 mm from the surface to 460 m and 300 mm from 460 m to 520 m.

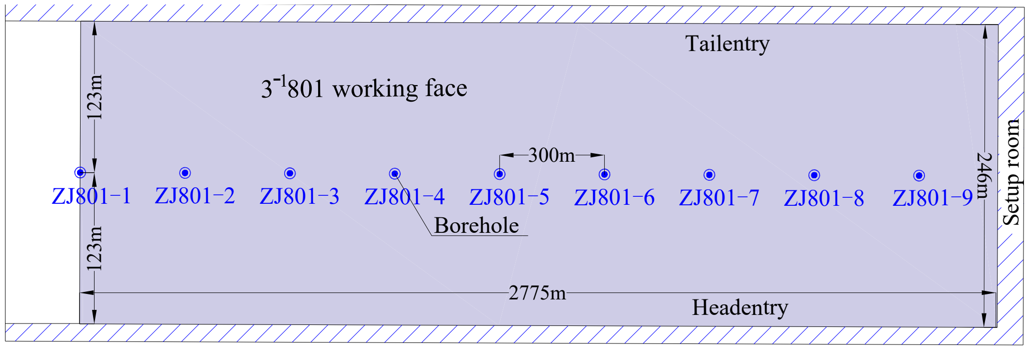

Figure 13. Location of the grouting boreholes.

5.2. Monitoring of Backfilling Effect

The monitoring of backfill grouting effect mainly consists of grout preparation monitoring, grout monitoring, and surface deformation monitoring as follows:

5.2.1. Monitoring of Slurry Preparation

The monitoring indices of the slurry preparation system mainly include the slurry content and particle sizes. The monitoring of the slurry content is usually realized by installing a slurry densimeter in a mixing tank and flowmeters in various supply pipelines, and installing weighing transducers in a belt conveyor to monitor ball milling quantities and amounts of material conveyed, eventually realizing the real-time monitoring of the slurry content. The monitoring of particle sizes involves first drying finished slurry product and then conducting sieve grading to determine the distribution of particles with an equivalent spherical diameter greater than 0.15 mm for coarse-grained gangues, and then using a dry laser particle size analyzer to measure the particle size distribution of fine-grained gangue.

5.2.2. Grouting Monitoring

Grouting monitoring mainly involves monitoring of grouting speed, grouting pressure, and the grouting quantity of single boreholes. The on-line monitoring of the grouting speed and the grouting quantity via single boreholes is mainly achieved by flow detection by installing slurry flowmeters in grouting pipelines. Piezometers are installed at grouting pumps and wellheads to realize on-line monitoring of grouting pump pressure and grouting pressure at each wellhead.

5.2.3. Surface Deformation Monitoring

As displayed in Figure 14, surface strata movement observation stations were arranged in eight horizontal mining zones. The measuring lines were arranged along the advance and dip directions of the working faces, among which, measuring line A strikes along the $3^{-1}801$ working face, measuring line B strikes along the 3-1802 working face, and measuring line C strikes along the dip direction of the coal working face (the spacing between measuring points was 25 m).

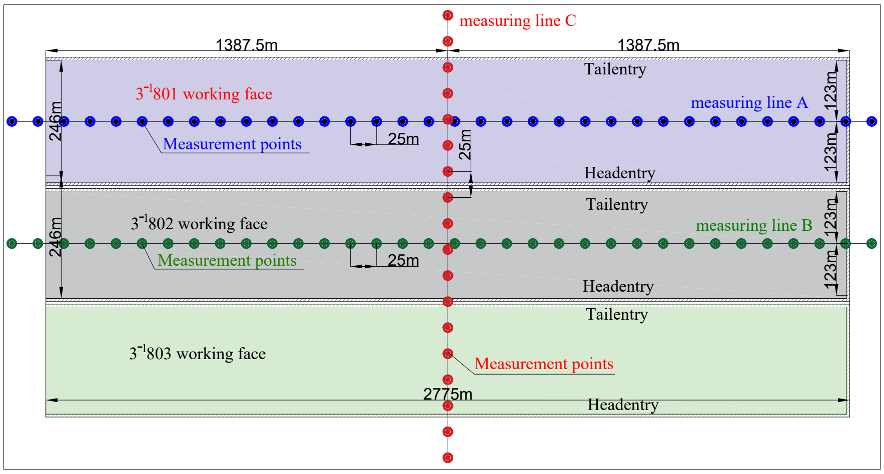

Figure 14. Layout of observation station of surface strata movement.

5.3. Field Measurement Analysis of Backfilling Effect

5.3.1. Field Measurement of Slurry Preparation Effect

The slurry content is calculated using Equation (18)

$$N = \frac{Q_g}{Q_g + Q_w}, \tag{18}$$

where, N is the slurry content, Q_g denotes the mass of crushed gangue, and Q_w is the mass of water added. According to field measurements, the average slurry content is about 58% and the average slurry density is about 1.38 g/cm^3, which is close to the designed values.

5.3.2. Field Measurement of Backfill Grouting Effect

① Grouting pressure

Taking the No. 3 borehole as an example, the grouting pressure is shown in Figure 15.

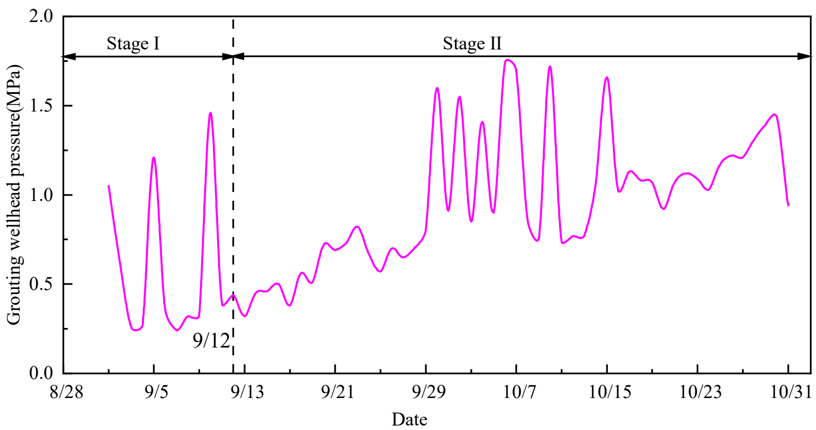

Figure 15. Grouting wellhead pressure measurement chart.

As illustrated in Figure 15, pressure fluctuations are large during Stage-I grouting; however, the average grouting pressure generally stabilizes; during Stage-II grouting, the grouting pressure stills fluctuate significantly, the overall pressure tends to rise; however, the pressure in the subsequent space tends to stabilize because the $3^{-1}801$ working face is grouted after being mined out. Hence, the phenomenon whereby the grouting pressure gradually rises with increasing grouting is mainly attributed to the sedimentation and accumulation of gangue slurry in the subsequent space. If rupture and subsidence occur in key strata, the subsequent space is subjected to significant compression. After injection of a small amount of slurry, the grouting pressure will rapidly increase to its maximum value within a short time. Hence, the monitoring results of the grouting pressure in the 3^{-1}801 working face show that key strata are not subjected to a large range of rupture and subsidence.

② Amount of grouting

Taking No. 3 borehole as an example, monitoring data pertaining to the amounts of slurry delivered are illustrated in Figure 16. In the early stages the grouting rate fluctuated, but the average rate still exceeded 150 t/h. After 7 October 2021, as grouting pressure had increased to a higher value, the grouting speed was slightly decreased, but was still maintained at more than 120 t/h. If key strata showed a large range of rupture and subsidence, the subsequent space would be compacted. This led to the difficulty in long-term injection of a large amount of slurry. The field measurement of grouting speed indicated that the average grouting speed of No. 3 borehole reached 156.9 t/h, indicating a rapid rate of grouting sustained for a long time and delivering a large volume of grout. This also verified that the primary reason for the increase of grouting pressure is slurry sedimentation and accumulation rather than rupture and subsidence of key strata.

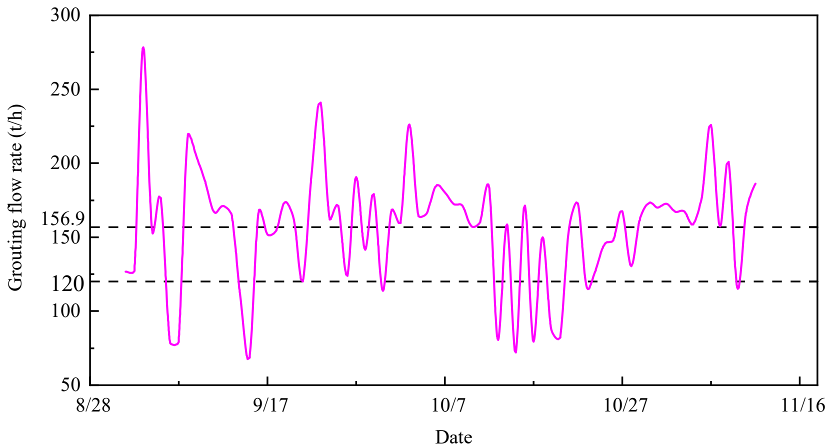

Figure 16. Grouting flow rate measurement chart.

5.3.3. Field Measurement of Surface Deformation

Surface subsidence was measured three months after the completion of mining at the working face. The dip length of the 3^{-1}101 and 3^{-1}801 working faces is 246 m, the advancing lengths of the working faces are 3211 m and 2775 m, respectively. Among which, the 3^{-1}101 working face was mined using the total caving method, which means that the EBR is 0%. As shown in Figures 17 and 18, the measured maximum subsidence of the dip and strike directions in the 3^{-1}101 working face is 1511 mm and 1535 mm, respectively. The extremum value of subsidence predicted using the proposed model is 1506 m (a maximum discrepancy of 1.9%). The 3^{-1}801 working face was subjected to backfill grouting in the mining process. Considering a certain safety coefficient, real grouting amount is 110,000 t and the EBR is 85%, the measured maximum surface subsidence of the dip and strike directions is 244 mm and 298 mm separately, the extreme value of subsidence predicted using the model is 289 m (a maximum discrepancy of 3.1%). The comparison of the surface subsidence for the two working faces suggests that the GGFSS technique has a beneficial effect on controlling the overburden strata on the goaf in the 3^{-1}801 working face, which plays an effective and protective role in key strata. This reduces the bending subsidence of overburden strata, reflecting in decreased surface subsidence.

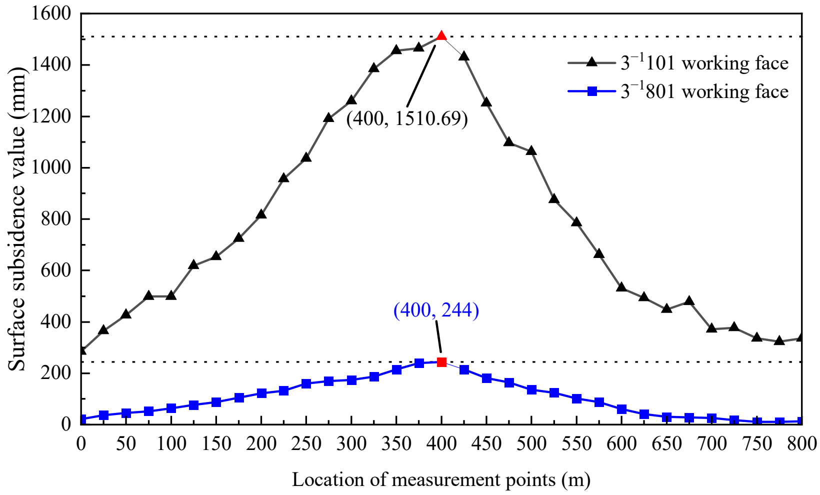

Figure 17. Surface subsidence along the dip direction of the working face.

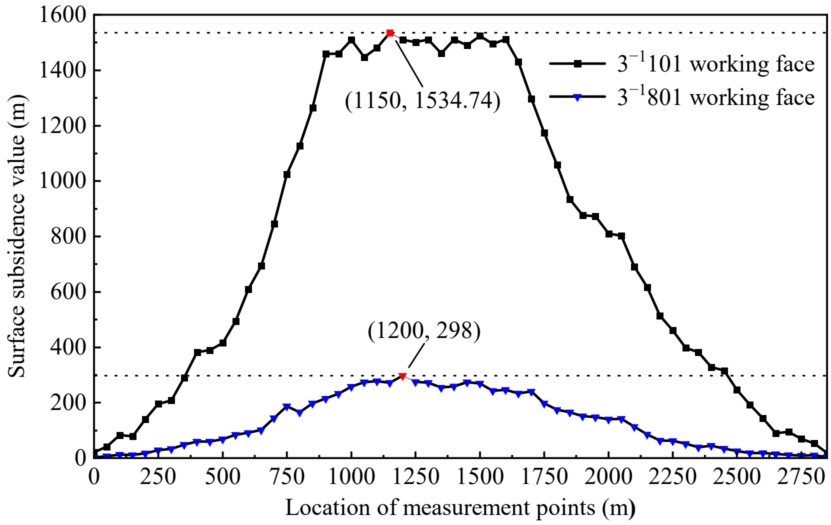

Figure 18. Surface subsidence along the strike direction of the working face.

As shown in Figure 19, as the backfill grouting begins, the surface subsidence rate of the $3^{-1}801$ working face slows to a remarkable extent, indicating that the backfill slurry has filled the subsequent space, controlling the movement of overburden strata and further reducing the rate of surface subsidence.

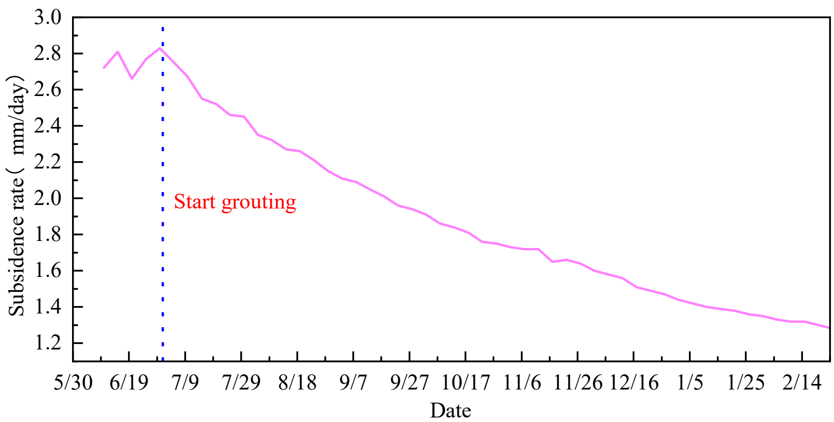

Figure 19. Rate of surface subsidence before and after GGFSS.

6. Conclusions

The paper aims to fill the gaps of other filling methods such as solid filling and paste filling and proposes a high-productivity and high-efficiency filling method that can be applied in high-capacity mines. This paper firstly explains the principle and technical key of GGFSS technology in coal mining, proposes the EBR mechanical model, and establishes the GGFSS rock control mechanical model based on this, and based on the probability integral method surface deformation prediction model, proposes the GGFSS surface deformation prediction model, and finally the application effect for GGFSS project is measured and analyzed.

(1) This research elucidated technical principles and advantages of the GGFSS technique. Based on the general concept underpinning this technique, the connotation, and a formula for the calculation, of the EBR were proposed to explore the primary factors influencing the EBRs. On this basis, an EBR mechanical model was established based on the Winkler foundation theory.
(2) The analysis of the established EBR-based strata movement mechanical model indicates that: the subsidence and bending moment of key strata both are decreased with increasing EBR; and when the EBR is greater than 74.44%, key strata remain free from rupture and their subsidence is significantly reduced.
(3) Based on the EBR, a predictive model of surface deformation when using GGFSS was constructed. The surface deformation predictions show that: as the EBR is increased from 70% to 75%, deformation indices including surface subsidence show significant and rapid reductions. Thereafter, with the increase in the EBR, the decrease of surface deformation slows, given a certain allowance coefficient, the EBR was designed to be 85% herein.
(4) The designed backfill grouting layer in the subsequent space is located at the water-resisting key stratum 131 m above coal seams, with a backfill grouting borehole spacing of 300 m. The designed slurry mass concentration is 60%, one-third of the gangue crushed to a diameter below 2 mm, and two-thirds of the gangue crushed to a diameter below 0.15 mm. Field measurement results indicate that: the surface subsidence is close to that predicted using the proposed model, with an average rate of grouting of 156.9 t/h, sustained for a long time and delivering a large volume of grouting slurry; the grouting pressure shows no rapid increases at the grouting wellhead, implying that key strata remain largely free from rupture. The surface deformation results indicated that GGFSS significantly reduces surface subsidence.

Subsequent in-depth study will focus on the structural characteristics and spatiotemporal evolution of pores in the subsequent space, which is the difficulty and technical key of the GGFSS. The accurate evaluation of filling space, reasonable layout of filling hole and diffusion law of filling slurry are all closely related to the spatial pore distribution of the subsequent space.

Author Contributions: Conceptualization, J.Z. and T.A.; methodology, Z.W. and T.A.; software, Z.W.; validation, Y.L. and H.Y.; formal analysis, T.A. and N.Z.; investigation, Y.L. and G.D.; resources, T.A.; data curation, Z.W.; writing—original draft preparation, Z.W. and G.D.; writing—review and editing, J.Z., H.Y. and N.Z.; visualization, T.A.; supervision, J.Z. All authors have read and agreed to the published version of the manuscript.

Funding: This work was supported by the National Natural Science Foundation of China [grant number 52130402].

Data Availability Statement: Not applicable.

Conflicts of Interest: The authors declare no conflict of interest.

References

1. Yao, Y.; Deng, Q.; Li, Y.; Lu, H.; Zou, R. Comprehensive treatment of coal gangue and its development and utilization status. *China Resour. Compr. Util.* **2019**, *37*, 83–85.
2. Chen, Q.; Zhang, Q.; Qi, C.; Fourie, A.; Xiao, C. Recycling phosphogypsum and construction demolition waste for cemented paste backfill and its environmental impact. *J. Clean. Prod.* **2018**, *186*, 418–429. [CrossRef]
3. Zhang, J.; Zhang, J.; Spearinga, A.J.S.; Miao, X.; Guo, S.; Sun, Q. Green coal mining technique integrating mining-dressing-gas draining-backfilling-mining. *Int. J. Min. Sci. Technol.* **2017**, *27*, 17–27. [CrossRef]
4. Hu, B.; Liu, P.; Cui, F.; Wang, H. Review and development status of backfill coal mining technology in China. *Coal Sci. Technol.* **2020**, *40*, 18.
5. Sun, Q.; Zhang, J.; Zhou, N.; Huang, Y. Key Aquiclude Strata Reconstruction and Fluid-Solid Coupled Deformation Mechanism Study for Backfill Coal Mining. *Mine Water Environ.* **2021**, *40*, 793–802. [CrossRef]
6. Yan, H.; Zhang, J.; Zhou, N.; Zhang, S.; Dong, X. Shaft failure characteristics and the control effects of backfill body compression ratio at ultra-contiguous coal seams mining. *Environ. Earth Sci.* **2018**, *77*, 458. [CrossRef]
7. Liu, Y.; Liu, J.; Yang, B.; Yuan, S. Assessing Water and Sand Inrushes Hazard Reductions due to Backfill Mining by Combining GIS and Entropy Methods. *Mine Water Environ. J. Int. Mine Water Assoc.* **2021**, *40*, 956–969. [CrossRef]
8. Zhou, N.; Zhang, J.; Yan, H.; Li, M. Deformation Behavior of Hard Roofs in Solid Backfill Coal Mining Using Physical Models. *Energies* **2017**, *10*, 557. [CrossRef]
9. Gu, W.; Zhu, L.; Liu, Z.; Song, T.; Pan, H.; Zhang, X.; Qiu, F.; Zhao, M.; Huang, J. Fluidization slurry backfilling technology of coal mine solid waste. *Coal Sci. Technol.* **2021**, *49*, 83–91. [CrossRef]
10. Yang, K.; Zhao, X.; Wei, Z.; Zhang, J. Development overview of paste backfill technology in China's coal mines: A review. *Environ. Sci. Pollut. Res.* **2021**, *28*, 67957–67969. [CrossRef]
11. Deng, X.; Yuan, Z.; Lan, L.; Wit, B.D.; Zhang, J. Roof Movement and Failure Behavior When Mining Extra-Thick Coal Seams Using Upward Slicing Longwall-Roadway Cemented Backfill Technology. *Adv. Mater. Sci. Eng.* **2020**, *2020*, 5828514. [CrossRef]
12. Zhang, J.; Li, M.; Taheri, A.; Zhang, W.; Wu, Z.; Song, W. Properties and Application of Backfill Materials in Coal Mines in China. *Minerals* **2019**, *9*, 53. [CrossRef]
13. Xu, Y.; Ma, L.; Ngo, I.; Zhai, J. Continuous Extraction and Continuous Backfill Mining Method Using Carbon Dioxide Mineralized Filling Body to Preserve Shallow Water in Northwest China. *Energies* **2022**, *15*, 3614. [CrossRef]
14. Deng, X.; Li, Y.; Wang, F.; Shi, X.; Yang, Y.; Xu, X.; Huang, Y.; Wit, B.D.; University, T. Experimental study on the mechanical properties and consolidation mechanism of microbial grouted backfill. *Int. J. Min. Sci. Technol.* **2022**, *32*, 271–282. [CrossRef]
15. Zhang, J.; Zhang, Q.; Zhou, N.; Li, M.; Huang, P.; Li, B. Research progress and prospect of coal based solid waste backfilling mining technology. *J. China Coal Soc.* **2022**, *47*, 4167–4181. [CrossRef]
16. Li, B.; Zhang, J.; Ghoreishi-Madiseh, S.A.; Brito, M.; Kuyuk, A.F. Energy performance of seasonal thermal energy storage in underground backfilled stopes of coal mines from China. *J. Clean. Prod.* **2020**, *275*, 122647. [CrossRef]
17. Qi, C.; Tang, X.; Dong, X.; Chen, Q.; Fourie, A.; Liu, E. Towards Intelligent Mining for Backfill: A genetic programming-based method for strength forecasting of cemented paste backfill. *Miner. Eng.* **2019**, *133*, 69–79. [CrossRef]
18. Huang, Y.; Li, J.; Song, T.; Kong, G.; Li, M. Analysis on Filling Ratio and Shield Supporting Pressure for Overburden Movement Control in Coal Mining with Compacted Backfilling. *Energies* **2016**, *10*, 31. [CrossRef]
19. Huang, P. Study on control effect of roof based on backfilling body cooperating with support. *J. Min. Sci.* **2020**, *37*, 128–136.
20. Zhang, Q.; Chang-Long, D.U.; Zhang, J.X.; Wang, J.Q.; Meng, L.I.; Wen-Yue, Q.I. Backfill support's backfill and operation properties and evaluation. *J. Cent. South Univ.* **2018**, *25*, 1524–1534. [CrossRef]
21. Vu, T.T. Solutions to prevent face spall and roof falling in fully mechanized longwall at underground mines, Vietnam. *Min. Miner. Depos.* **2022**, *16*, 127–134. [CrossRef]
22. Dychkovskyi, R.; Shavarskyi, I.; Saik, P.; Lozynskyi, V.; Falshtynskyi, V.; Cabana, E. Research into stress-strain state of the rock mass condition in the process of the operation of double-unit longwalls. *Min. Miner. Depos.* **2020**, *14*, 85–94. [CrossRef]
23. Smoliński, A.; Malashkevych, D.; Petlovanyi, M.; Rysbekov, K.; Lozynskyi, V.; Sai, K. Research into Impact of Leaving Waste Rocks in the Mined-Out Space on the Geomechanical State of the Rock Mass Surrounding the Longwall Face. *Energies* **2022**, *15*, 9522. [CrossRef]
24. Malashkevych, D.; Petlovanyi, M.; Sai, K.; Zubko, S. Research into the coal quality with a new selective mining technology of the waste rock accumulation in the mined-out area. *Min. Miner. Depos.* **2022**, *16*, 103–114. [CrossRef]
25. Yan, H.; Wang, W.; Zhang, J.; Ma, D.; Zhou, N.; Wan, Z. Experimental study on the influence of coal-rock interface strength on crack propagation law of supercritical carbon dioxide fracturing. *Gas Sci. Eng.* **2023**, *112*, 204943. [CrossRef]
26. Xu, J.L.; Xuan, D.Y.; Zhu, W.B.; Wang, X.Z.; Teng, H. Study and application of coal mining with partial backfilling. *Meitan Xuebao/J. China Coal Soc.* **2015**, *40*, 1303–1312.
27. Chang, Q.L.; Zhou, H.Q.; Bai, J.B.; Duan, C.R.; Li, Y.W. Stability study and practice of overlying strata with paste backfilling. *J. Min. Saf. Eng.* **2011**, *28*, 279–282.
28. Meng-Tang, H.U.; Zhang, D.S.; Li-Jiang, M.A.; Wang, X.F.; Zhang, W. Roof control technology for longwall filling mining of superhigh-water material. *Meitan Xuebao J. China Coal Soc.* **2014**, *39*, 410–416.
29. Guo, G.-L.; Zhu, X.-J.; Zha, H.-F.; Wang, Q. Subsidence prediction method based on equivalent mining height theory for solid backfilling mining. *Trans. Nonferr. Met. Soc. China* **2014**, *24*, 3302–3308. [CrossRef]

30. Zhu, X.; Guo, G.; Liu, H.; Yang, X. Surface subsidence prediction method of backfill-strip mining in coal mining. *Bull. Eng. Geol. Environ.* **2019**, *78*, 6235–6248. [CrossRef]
31. Wang, L.; Zhang, X.N.; Guo, G.L.; Zha, J.F. Research on surface subsidence prediction model of coal mining with solid compacted backfilling. *Yantu Lixue/Rock Soil Mech.* **2014**, *35*, 1973–1978.
32. Yin, W.; Bao, X.; Liu, H.; Zhang, Q. Research on overlying strata structure and ground control in transition area of fully mechanized mining working face. *Caikuang Yu Anquan Gongcheng Xuebao J. Min. Saf. Eng.* **2018**, *35*, 86–93. [CrossRef]
33. Zhang, Q.; Cui, P.; Zhang, J.; Zhang, H.; Chang, T.; Yang, J. Condition state characterization and self-identification control method of key equipment for intelligent solid backfilling. *Meitan Xuebao* **2022**, *47*, 4237–4249. [CrossRef]
34. Tran, V. Using Artificial Intelligence Approach for Investigating and Predicting Yield Stress of Cemented Paste Backfill. *Sustainability* **2023**, *15*, 2892. [CrossRef]
35. Behera, S.K.; Mishra, D.P.; Singh, P.; Mishra, K.; Mandal, S.K.; Ghosh, C.N.; Kumar, R.; Mandal, P.K. Utilization of mill tailings, fly ash and slag as mine paste backfill material: Review and future perspective. *Constr. Build. Mater.* **2021**, *309*, 125120. [CrossRef]
36. Qi, C.C.; Fourie, A. Cemented paste backfill for mineral tailings management: Review and future perspectives. *Miner. Eng.* **2019**, *144*, 106025. [CrossRef]
37. Li, L.; Huang, Q.; Zuo, X.; Wu, J.; Wei, B.; He, Y.; Zhang, W.; Zhang, J. Study on the Slurry Diffusion Law of Fluidized Filling Gangue in the Caving Goaf of Thick Coal Seam Fully Mechanized Caving Mining. *Energies* **2022**, *15*, 8164. [CrossRef]
38. Zhu, L.; Pan, H.; Gu, W.; Zhao, M.; Zhang, X.; Xu, K. Experimental study on flow and diffusion law of gangue filling slurry in caving zone. *Meitan Xuebao* **2021**, *46*, 629–638. [CrossRef]